MATERIALS PHYSICS AND MECHANICS RESEACH ARTICLE

Submitted: November 3, 2023 **Revised: November 30, 2023** **Accepted: December 9, 2023**

Emission of lattice dislocations from triple junctions of grain boundaries in high-temperature ceramics with amorphous intercrystalline layers

M.Yu. Gutkin, **N.V. Skiba** ✉,

Institute for Problems in Mechanical Engineering RAS, St. Petersburg, Russian Federation

✉ nikolay.skiba@gmail.com

ABSTRACT

A theoretical model of a mechanism of plastic deformation in high-temperature ceramic materials containing amorphous intercrystalline layers (AILs) is suggested. Within the model, the plastic deformation is realized due to the nucleation and the development of inclusions of a liquid-like phase in the AILs and the glide of lattice dislocations emitted from the triple junctions of the AILs that contain the liquid-like phase inclusions. In the exemplary case of high-temperature α-Al_2O_3 ceramics with AILs, the temperature dependences of the critical stresses for the formation of a liquid-like phase nucleus, for the lattice dislocation emission and for the lattice dislocation glide in a wide range of the deformation temperatures from 300 to 1500 K are calculated. The critical values of the external shear stress and the deformation temperature, at which the glide of the emitted lattice dislocations in the grain interior becomes energetically favorable, are determined.

KEYWORDS

high-temperature ceramics • amorphous intercrystalline layers • liquid-like phase inclusions lattice dislocations • deformation temperature

Acknowledgements. *The authors gratefully appreciate the Russian Science Foundation for financial support of this study (grant №23-19-00236).*

Citation: Gutkin MYu, Skiba NV. Emission of lattice dislocations from triple junctions of grain boundaries in high-temperature ceramics with amorphous intercrystalline layers. *Materials Physics and Mechanics*. 2024;52(1): 39-48. http://dx.doi.org/10.18149/MPM.5212024_4

Introduction

It is well known that high-temperature ceramic materials and composites have high strength, hardness and wear resistance, maintaining these characteristics at elevated temperatures [1–3]. These unique properties depend on the deformation behavior of intercrystalline boundaries. According to experimental data [4–6], the grain boundaries in the ceramic materials with covalent chemical bonding (Al_2O_3, SiC, Si_3N_4, etc.) often contain amorphous intercrystalline layers (AILs), which have an approximately constant thickness (of the order of several nanometers). The experimental observations of the nucleation and the evolution of the AILs are difficult due to their small size that stimulated the development of analytical theoretical models [7–9] and computer modeling [10–13] of the deformation behavior of intercrystalline boundaries.

In particular, in the works [10–12] on computer modeling of amorphous silicon, it was shown that the material is divided into two phases: a solid-like matrix and regions of a liquid-like phase. According to these models [10–12], the liquid-like phase regions are the carriers of plastic deformation in amorphous silicon and their volume fraction increases

Publisher: Peter the Great St. Petersburg Polytechnic University

under mechanical loading. Also, the authors of the work [11] came to the conclusion that a similar mechanism of plastic deformation can operate in other amorphous materials with covalent bonds.

Based on the results of computer modeling [10–12], a mechanism of plastic deformation in nanoceramics with AILs through the nucleation and evolution of liquid-like inclusions in the grain boundaries under the action of an external shear stress was considered in analytical theoretical models [7–9]. The plastic shear within the liquid-like inclusions and their elastic fields and energies were modeled by gliding dislocation loops [7,8] and dislocation dipoles [9] with increasing Burgers vectors. Within the framework of these models, the achievement of a certain critical value by the external shear stress led to the formation of a liquid-like nucleus that grew in size and filled the entire grain boundary between the adjacent triple junctions. Also, in theoretical works [8,9], two cases of further development of plastic deformation in the nanoceramics with AILs were considered: (i) due to the nucleation of nanocracks on the liquid-like phase inclusions and the propagation of these nanocracks in the neighboring AILs [8], and (ii) due to liquid-like phase inclusions overcoming the triple junctions of the AILs and penetrating into a neighboring AIL [9].

The main aim of this work is to propose the third possible scenario for the development of plastic deformation in the high-temperature ceramics with AILs due to the nucleation and the extension of the liquid-like phase inclusions in the AILs with the subsequent emission of lattice dislocations from the triple junctions of the AILs and the glide of these dislocations into the bulk of a neighboring grain. As a result of this model, the critical values of the external shear stress that are required for the formation of a liquid-like nuclei, for the lattice dislocation emission from the triple junctions, and for the lattice dislocation glide in the grain interiors in a wide temperature range in the exemplary case of a high-temperature α-Al_2O_3 ceramics with the AILs are estimated and discussed in detail.

Model

Within the framework of the approach used in the model [9], a ceramic sample consists of crystallites divided by the AILs (Fig. 1(a)). Consider an individual AIL AC with length L and width h, in which acts the maximum shear stress $\tau = \sigma/2$ resulting from the application of an external mechanical tensile stress σ (Fig. 1(b)).

According to the works [8,9], a nucleus of a liquid-like phase of length l starts to form in the AIL when the external shear stress reaches a certain critical value $\tau = \tau_{c1}$ (Fig. 1(b)). This nucleus of the liquid-like phase is a carrier of the plastic shear s that is modeled by an edge dislocation dipole with the variable Burgers vectors $\pm\mathbf{s}$ ($\pm s$-dislocation dipole) and the arm l (Fig. 1(b)). Under the action of the external shear stress $\tau \geq \tau_{c1}$, the nucleus grows and transforms into an inclusion of length L, which corresponds to the length of AIL AC, with a simultaneous increase in the plastic shear value s, which is described by an increase in the strength of the $\pm s$-dislocation dipole to a certain value B (Fig. 1(c)). As a result, the defect structure is characterized by a dipole of superdislocations with Burgers vectors $\pm\mathbf{B}$ ($\pm B$-superdislocation dipole) and arm L (Fig. 1(c)).

Further, it is assumed that, under the combine action of the external shear stress $\tau \geq \tau_{c2}$ and the stress field of the $\pm B$-superdislocation dipole, a lattice dislocation (LD) with the Burgers vector **b** (b-LD) is emitted from triple junction C of the AILs into the adjacent grain interior under the angle α to AC plane (Fig. 1(d)). Here τ_{c2} denotes a critical value of the external shear stress τ, at which the emission of the LD becomes energetically favorable. Upon reaching a critical stress τ_{c3} that determines the shear stress required to overcome the Peierls barrier, the emitted LD can glide over the distance p along its easy slip plane (Fig. 1(d)). In the model, the b-LD emission is modeled by the formation of a LD dipole with the Burgers vectors $\pm$**b** ($\pm b$-LD dipole) (Fig. 1(d)). It is worth noting that a similar model was invented long ago by Pozdnyakov and Glezer [14] although without thorough examination.

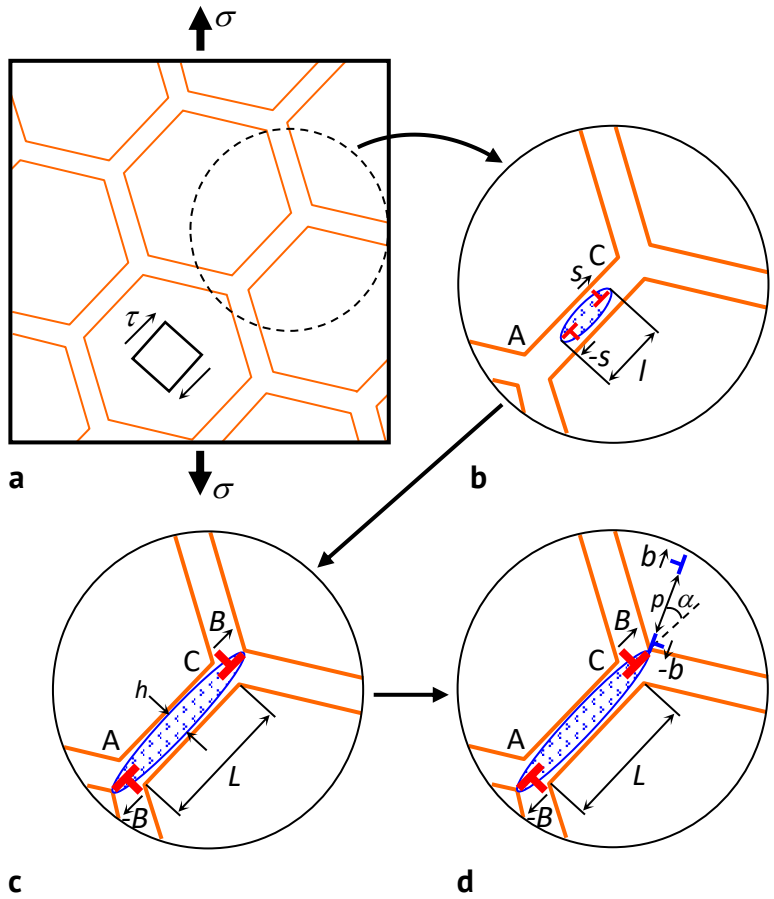

Fig. 1. A two-dimensional model of the plastic deformation of ceramics with AILs.
(a) Model of a ceramic sample with AILs under mechanical tensile stress σ.
(b) An individual AIL AC with a nucleus of the liquid-like phase, modeled by an ellipsoidal inclusion that contains an edge dislocation dipole with growing Burgers vectors $\pm$**s**. (c) Growth of the liquid-like phase inclusion with the dipole of superdislocations with Burgers vectors $\pm$**B** to the size L. (d) Emission of a lattice dislocation with the Burgers vector **b** from triple junction C of the AILs into an adjacent grain under the angle α to AC plane and the dislocation glide in the grain interior over the distance p

Thus, it is assumed that the glide of LDs emitted from the triple junctions of AILs can provide the development of plastic deformation in the case when further evolution of the liquid-like inclusions is suppressed.

Results

Consider the energy characteristics of the formation of a liquid-like phase nucleus in AIL AC, which contains a $\pm s$-dislocation dipole with variable Burgers vectors (Fig. 1(a-c)).

The change in the total energy of the system ΔW that characterizes the formation of the $\pm s$-dislocation dipole surrounded by a region of the liquid-like phase is given by [9]:

$$\Delta W = E_d + \Delta HS - \tau\, sp, \tag{1}$$

where E_d is the strain energy of the $\pm s$-dislocation dipole; ΔH is the excess enthalpy of the liquid-like phase in comparison with the solid-like phase, and S is the cross-sectional area of the liquid-like phase nucleus.

The strain energy E_d of the $\pm s$-dislocation dipole reads [15,16]:

$$E_d = Ds^2\, ln\frac{l-r_c}{r_c}, \tag{2}$$

where $D = G/[2\pi(1-\nu)]$, G is the shear modulus, ν is the Poisson ratio, $r_c \approx s$ is the cutoff radius of the elastic field of the $\pm s$-dislocation dipole at the dislocation lines.

According to the work [9], the cross-sectional area $S = lh$, where $h \approx ka$ is the transverse size of the liquid-like phase nucleus, $k = (2...4)a$, a is the average interatomic distance within the AIL.

As a result, Eq. (1) for the energy change ΔW can be rewritten as follows:

$$\Delta W = \frac{Gs^2}{2\pi(1-\nu)}\, ln\frac{l-r_c}{r_c} + H\, lka - \tau\, sp. \tag{3}$$

With using Eq. (3), the maps of the energy change ΔW in the normalized coordinates s/a and l/a in the exemplary case of high-temperature α-Al_2O_3 ceramics at the different deformation temperatures T = 300 and 1500 K were calculated. To the best of our knowledge, no studies have been carried out until now to calculate the parameters characterizing the liquid-like phase in AILs in the α-Al_2O_3 ceramics. Therefore, in the first approximation, it is assumed that the elastic moduli of the liquid-like phase are approximately equal to those of the solid-like phase ($G_i = G_m = G$, $\nu_i = \nu_m = \nu$), weakly depend on the deformation temperature, and have the following values: G = 169 GPa and ν = 0.23 [17,18]. Also, in the absence of the calculations of the enthalpy values for the liquid-like phase, one can use the estimate $\Delta H_i \approx 1.5\Delta H_m$. This is motivated by the case of amorphous silicon (Si), in which the enthalpy of the liquid-like phase is approximately 1.5 times greater than the enthalpy of the solid-like phase both at low (T = 300 K) and high (T = 1000 K) temperatures [7]. Following the experimental work [19], the enthalpy ΔH_m of the solid-like phase is 10 kJ/mol at T = 300 K and 152.27 kJ/mol at T = 1500 K. As a result, the excess enthalpy $\Delta H = \Delta H_i - \Delta H_m \approx 0.05$ eV/at. at T = 300 K and 0.79 eV/at. at T = 1500 K. The average interatomic distance a in AILs, the magnitude of the LD Burgers vector b in the grain, and the transverse size h of the liquid-like phase nucleus in an AIL were chosen as follows, respectively: $a \approx 0.19$ nm, $b \approx 0.27$ nm [17], and $h \approx 2a$. The angle α was taken as the average angle α = 22° between 0 and 45° that correspond to the maximum and minimum levels of the external shear stress τ, respectively.

The results of numerical calculations of the maps of energy change ΔW in the normalized coordinates s/a and l/a are shown in Fig. 2(a) for the low deformation temperature (T = 300 K) and Fig. 2(b) for the high deformation temperature (T = 1500 K). In both the cases, the energy maps were built for the critical value τ_{c1} of the external shear stress τ, which characterizes the barrier-free formation of the liquid-like phase nucleus and

is approximately equal to 5.5 GPa for T = 300 K and 10.2 GPa for T = 1500 K. In these maps, the transition to the barrier-free regime of the nucleation of the liquid-like phase nucleus corresponds to the zero level ($\Delta W = 0$) contours touching the straight line $l = 2a$ that corresponds to the initial size of the liquid-like nucleus (Fig. 2). The arrows in Fig. 2, drawn from the nucleation point along the line of the maximum gradient of the function $\Delta W(s, l)$, indicate the evolution of both the liquid-like nucleus and $\pm s$-dislocation dipole in the space (s, l) under the critical stress τ_{c1}. As follows from Fig. 2, at both the low and high deformation temperatures, an increase in the length l of the liquid-like nucleus is accompanied by a corresponding increase in the strength s of the dislocation dipole, which reaches the value $s \approx 2.5a$ at T = 300 K (Fig. 2(a)) and $\approx 7.5a$ at T = 1500 K (Fig. 2(b)) when $l = 100a$. Using these relations, one can express the strength s of the dislocation dipole in terms of its arm l as follow: $s \approx 0.025l$ at T = 300 K and $\approx 0.075l$ at T = 1500 K.

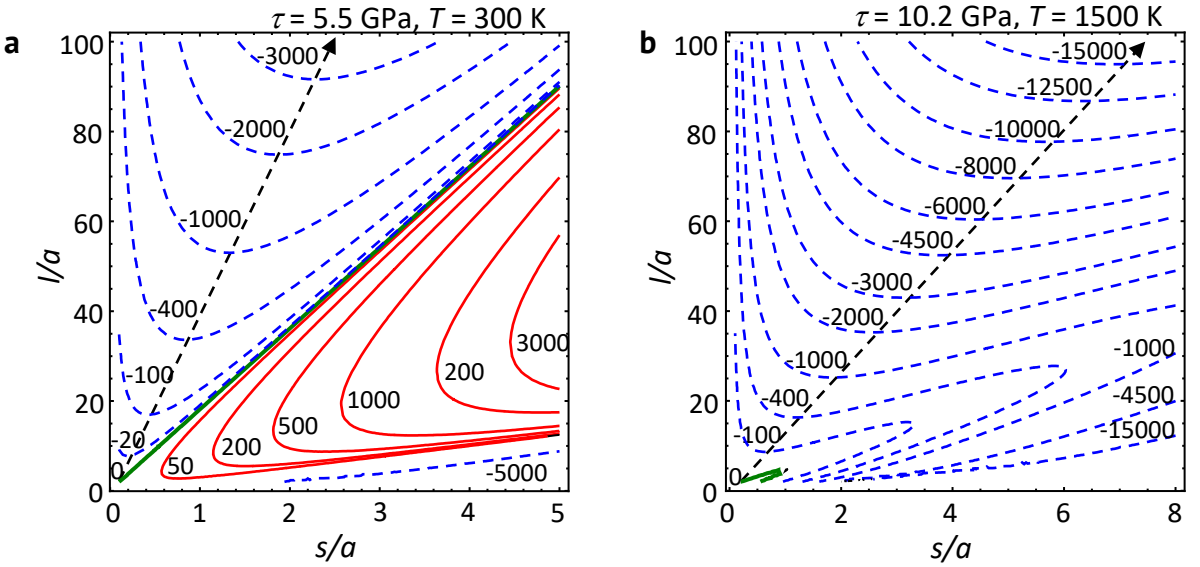

Fig. 2. Contour maps of the energy change ΔW (in units of eV/nm) in the space of the normalized strength s/a and the normalized arm l/a of the $\pm s$-dislocation dipole at the deformation temperature T = (a) 300 and (b) 1500 K, and at the external shear stress τ = (a) 5.5 and (b) 10.2 GPa

Let us consider now the energy characteristics that correspond to the LD emission from the triple junction of AILs at point C (Fig. 1(d)). It is assumed that, under the action of the external shear stress $\tau \geq \tau_{c1}$, the liquid-like phase inclusion fills entire AIL AC, thus increasing in size to the length $l = L$, and the $\pm s$-dislocation dipole (modeling the plastic shear associated with the growth of the liquid-like phase inclusion) is transformed into the $\pm B$-superdislocation dipole (Fig. 1(c)).

The process of the LD emission is specified by the energy change $\Delta W_b = W_{b2} - W_{b1}$, where W_{b1} and W_{b2} are the energies of the system in the initial state, before the b-LD emission (Fig. 1(c)), and in its current state, after the b-LD emission and glide over a distance p (Fig. 1(d)), respectively. Such a transformation of the defect system is energetically favorable if $\Delta W_b < 0$.

The energy change ΔW_b (per unit length of the b-LD) can be written as follows:

$$\Delta W_b = E_b + E_{int} - \tau bp, \qquad (4)$$

where E_b is the self energy of the $\pm b$-LD dipole, E_{int} is the interaction energy between the $\pm B$-superdislocation dipole and the $\pm b$-LD dipole, and p is the distance moved by the emitted b-LD in the grain interior.

The self energy E_b of the $\pm b$-LD dipole is given by [15,16]:

$$E_b = Db^2\left(ln\frac{p-r_b}{r_b}+1\right), \tag{5}$$

where $r_b \approx b$.

The interaction energy E_{int} is calculated by a standard method [15,16] as the work spent to generate the $\pm b$-LD dipole in the stress field of the $\pm B$-superdislocation dipole. After some algebra, it reads:

$$E_{int} = \frac{DBb}{2}\left(cos\,\alpha\left(ln\frac{L^2+p^2+2Lp\,cos\,\alpha}{L^2+b^2+2Lb\,cos\,\alpha} - 2\,ln\frac{p}{b}\right) - \frac{2Lp\,sin^2\,\alpha}{L^2+p^2+2Lp\,cos\,\alpha} + \frac{2Lb\,sin^2\,\alpha}{L^2+b^2+2Lb\,cos\,\alpha}\right). \tag{6}$$

Using Eqs. (4)-(6), the dependence of the energy change ΔW_b on the distance p was calculated for different values of the external shear stress τ and the size L of the liquid-like phase inclusions. The numerical calculation of the dependences $\Delta W_b(p)$ was carried out at the same values of the system parameters as before, in calculating the energy maps $\Delta W(s, l)$ shown in Fig. 2 in the exemplary case of the high-temperature α-Al_2O_3 ceramics with AILs. The strength B of the $\pm B$-superdislocation dipole was chosen equal to $\approx 0.025L$ at T = 300 K and $\approx 0.075L$ at T = 1500 K. The dependences $\Delta W_b(p)$ are shown in Figs. 3 and 4 for different values of the size L of the liquid-like phase inclusion: L = 5 (Figs. 3(a) and 4(a)), 10 (Figs. 3(b) and 4(b)), 15 (Figs. 3(c) and 4(c)), and 20 nm (Figs. 3(d) and 4(d)).

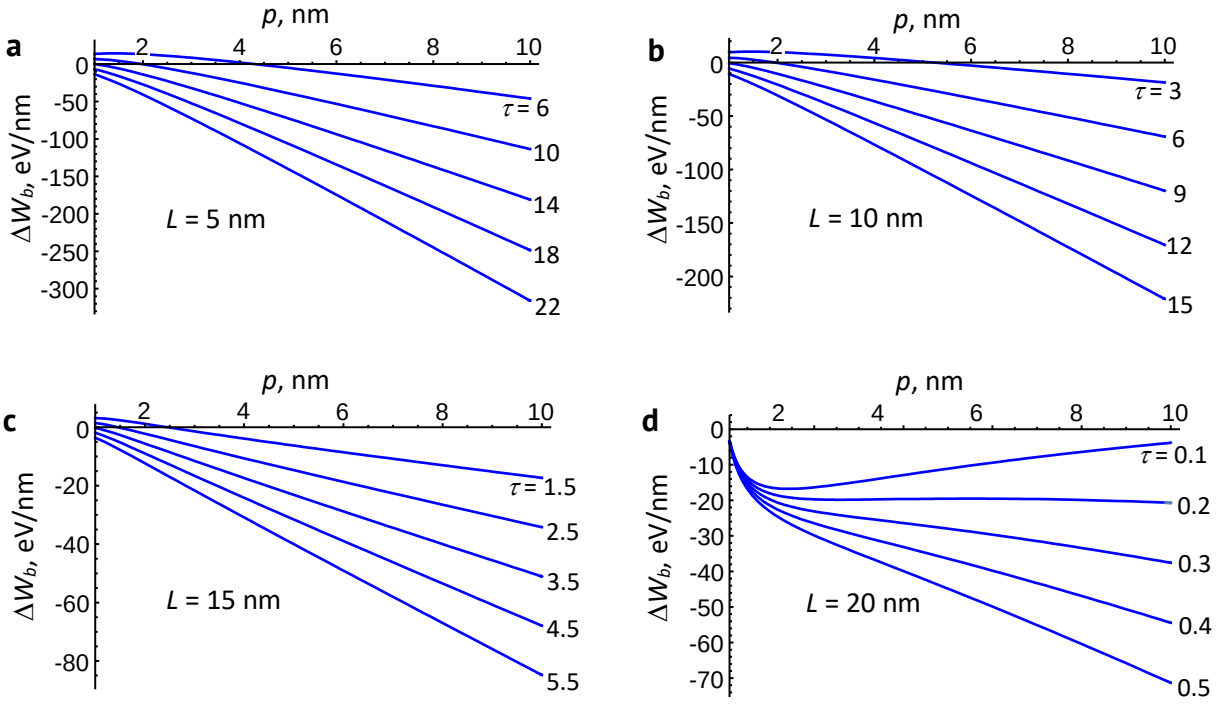

Fig. 3. Dependence of the energy change ΔW on the distance p at various values of the external shear stress τ (shown at curves in units of GPa) for different sizes L = (a) 5, (b) 10, (c) 15 and (d) 20 nm, in the case of low deformation temperature T = 300 K

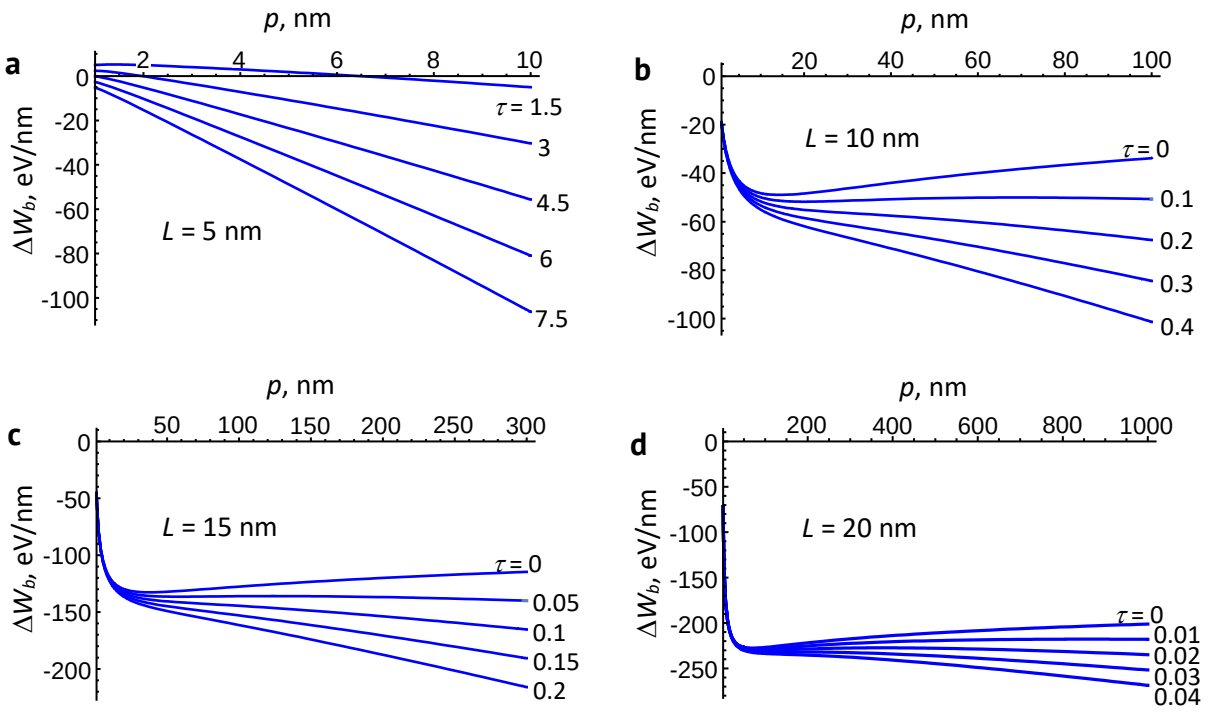

Fig. 4. Dependence of the energy change ΔW on the distance p at various values of the external shear stress τ (shown at curves in units of GPa) for different sizes L = (a) 5, (b) 10, (c) 15 and (d) 20 nm, in the case of high deformation temperature T = 1500 K

The emission of the LD and its subsequent glide in the grain interior is energetically favorable, if the energy change ΔW_b is negative at the initial point of the LD emission (when $p \approx 1$ nm) and then monotonously decreases with the distance p. In these circumstances, the critical stress τ_{c2} that is the minimum stress required for the emission of a LD from the triple junction of the AILs, can be calculated from the conditions $\Delta W_b \leqslant 0$ at $p = 1$ nm and $\partial \Delta W_b / \partial p < 0$ at $p > 1$ nm that guarantee the barrier-less emission of the LD.

As can be seen from the dependences $\Delta W_b(p)$ in Figs. 3 and 4, the critical stress τ_{c2} increases with a decrease in the length L of the liquid-like phase inclusion and a decrease in the deformation temperature T. For example, τ_{c2} = 14, 9, 3.5 and 0.3 GPa at T = 300 K (Fig. 3), and 4.5, 0.2, 0.1 and 0.03 GPa at T = 1500 K (Fig. 4) for the size L = 5, 10, 15 and 20 nm, respectively. The critical stresses τ_{c2} for other deformation temperatures in the range from 300 to 1500 K were determined in a similar way.

During its slip in the grain interior, the LD is subject to resistance from the crystal lattice that is characterized by the Peierls barrier. In this case, the LD slip becomes possible when the external shear stress τ reaches a certain critical value τ_{c3} that is required to overcome the Peierls barrier. The Peierls barrier depends on the temperature and decreases with an increase in it. Thus, the critical stress τ_{c3} also decreases with an increase in the temperature. The temperature dependences of the critical stresses τ_{c3b} and τ_{c3p} for the basal and prismatic slip, respectively, in α-Al_2O_3 ceramics were found in experiments [20]. They are given by the following formulas [20]:

$$\tau_{c3b} = \tau_{0b} e^{-0.0052\,T}, \quad (7)$$

$$\tau_{c3p} = \tau_{0p} e^{-0.0026T}, \quad (8)$$

where τ_{c0b} = 109 GPa and τ_{c0p} = 9 GPa.

With Eqs. (3)-(8), one can calculate the temperature dependences of the critical stresses τ_{c1}, τ_{c2}, and τ_{c3}. The resulting curves $\tau_{c1}(T)$, $\tau_{c2}(T)$, and $\tau_{c3}(T)$ are shown in Fig. 5 for different values of the size L of the liquid-like phase inclusion: L = 5 (Fig. 5(a)), 10 (Fig. 5(b)), 15 (Fig. 5(c)), and 20 nm (Fig. 5(d)). Within the model, the emission of LDs can occur only after the formation of a liquid-like phase inclusion. Therefore, the LD generation becomes energetically favorable if the conditions $\tau \geq \tau_{c1}$ and $\tau \geq \tau_{c2}$ are satisfied. In turn, the realization of the LD slip in the grain interior along its easy slip plane becomes possible if the conditions $\tau \geq \tau_{c3p}$ and/or $\tau \geq \tau_{c3b}$ are satisfied. Regions I and II correspond to the values of the external shear stress τ and the deformation temperature T, at which the glide of the LD along the basal (region I) and prismatic (region II) slip planes is possible (Fig. 5). As is seen from Fig. 5, the regions I and II expand with an increase in the size L of the liquid-like phase inclusions until this size reaches 15 nm and then rest constant in area.

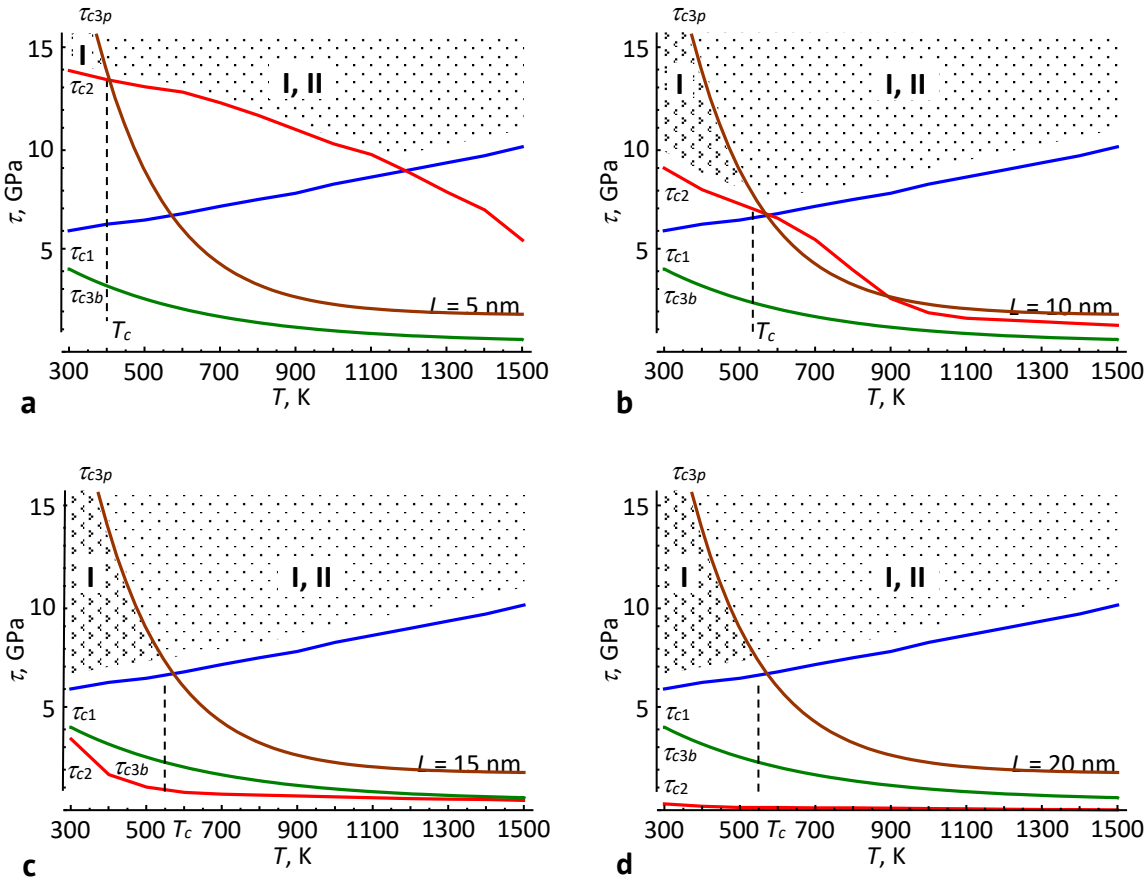

Fig. 5. Dependences of the critical stresses τ_{c1}, τ_{c2} and τ_{c3} on the deformation temperature T for different values of the liquid-like phase inclusion size L = (a) 5, (b) 10, (c) 15, and (d) 20 nm. Regions I and II correspond to the basal and prismatic plane slip, respectively

It should be noted that, as follows from Fig. 5, there is a certain critical deformation temperature T_c, below which the basal plane slip is possible at lower values of the external shear stress τ than those needed for the prismatic plane slip. When $T > T_c$, both the basal and prismatic slip systems are expected to be activated under the same shear stress $\tau \geq \max\{\tau_{c1}, \tau_{c2}\}$. The critical deformation temperature T_c increases with an increase

in the size L of the liquid-like phase inclusion up to a certain value $T_c \approx 550$ K, which is achieved at the size $L = 15$ nm in our exemplary case of the α-Al_2O_3 ceramics (Fig. 5(c)), while then it does not change with increasing L (Fig. 5(d)). As a result, the critical deformation temperature values vary with small L (when $5 \leqslant L \leqslant 15$ nm) in the range of $400 < T_c < 550$ K (Fig. 5).

Conclusions

Thus, a theoretical model of a new mechanism of plastic deformation in the high-temperature ceramics with amorphous intercrystalline layers over a wide temperature range is developed. Within the model, the plastic deformation of a ceramic sample has two stages.

At the first stage, the plastic deformation occurs due to the generation and the evolution of nuclei of the liquid-like phase in amorphous intercrystalline layers under the action of the external shear stress. This mechanism of plasticity works until the liquid-like phase inclusions reach the nearest obstacles that, in the case of nanoceramics, are the nearest triple junctions of amorphous intercrystalline layers.

At the second stage, the plastic deformation of the nanoceramic sample develops due to the emission of lattice dislocations from the liquid-like phase inclusions, inhibited by the triple junctions of amorphous intercrystalline layers, followed by the dislocation glide in the grain interior.

The energy characteristics of the generation of the liquid-like phase nuclei in the amorphous intercrystalline layers and the emission of the lattice dislocations from the triple junctions of amorphous intercrystalline layers containing the liquid-like phase inclusions are calculated. In the exemplary case of a high-temperature α-Al_2O_3 nanoceramics, the critical stresses for the formation of a liquid-like phase nucleus, for the emission of the lattice dislocations from the triple junctions of amorphous intercrystalline layers, and for the lattice dislocation glide along the basal and prismatic slip planes are calculated in dependence on the deformation temperature. The temperature dependences of these critical stresses are plotted for different sizes of the liquid-like phase inclusion. The ranges of the values of the external shear stress and the deformation temperature, at which the glide of the emitted lattice dislocations in the grain interior is energetically favorable, are determined. It is shown that there is a certain critical deformation temperature, below which the basal plane slip is more preferable than the prismatic plane slip. In the exemplary case of the high-temperature α-Al_2O_3 nanoceramics with amorphous intercrystalline layers, the critical deformation temperature increases from 400 to 550 K, when the size of the liquid-like phase inclusion increases from 5 to 15 nm, and then remains constant when this size grow further.

Thus, the plastic deformation of the high-temperature nanoceramics can effectively occurs through the emission of lattice dislocations from the triple junctions of amorphous intercrystalline layers at elevated temperatures.

References

1. Zhang D, Yu R, Feng X, Guo X, Yang Y, Xu X. Enhanced mechanical properties of Al_2O_3 nanoceramics via low temperature spark plasma sintering of amorphous powders. *Materials*. 2023;16(16): 5652.
2. Wang LY, An L, Zhao J, Shimai S, Mao XJ, Zhang J, Liu J, Wang SW. High-strength porous alumina ceramics prepared from stable wet foams. *J. Adv. Ceram*. 2021;10: 852–859.
3. Cheng M, Liu H, Zhao B, Huang C, Yao P, Wang B. Mechanical properties of two types of Al_2O_3/TiC ceramic cutting tool material at room and elevated temperatures. *Ceramics International*. 2017;43(16): 13869–13874.
4. Zhang ZL, Sigle W, Koch CT. Dynamic behavior of nanometer-scale amorphous intergranular film in silicon nitride by in situ high-resolution transmission electron microscopy. *Journal of the European Ceramic Society*. 2011;31(9): 1835–1840.
5. Subramaniam A, Koch CT, Cannon RM, Rühle M. Intergranular glassy films: An overview. *Materials Science and Engineering A*. 2006;422(1-2): 3–18.
6. Kleebe HJ. Structure and chemistry of interfaces in Si_3N_4 ceramics studied by transmission electron microscopy. *Journal of the Ceramic Society of Japan*. 1997;105(1222): 453–475.
7. Gutkin MYu, Ovid'ko IA. A composite model of the plastic flow of amorphous covalent materials. *Physics of the Solid State*. 2010;52(1): 58–64.
8. Gutkin MYu, Ovid'ko IA. Plastic flow and fracture of amorphous intercrystalline layers in ceramic nanocomposites. *Physics of the Solid State*. 2010;52(4): 718–727.
9. Gutkin MYu, Mikaelyan KN. A model of strain hardening in nanoceramics with amorphous intercrystalline layers. *Physics of Complex Systems*. 2021;2(2): 51–60.
10. Demkowicz MJ, Argon AS. High-density liquidlike component facilitates plastic flow in a model amorphous silicon system. *Physical Review Letters*. 2004;93(2): 025505.
11. Demkowicz MJ, Argon AS. Liquidlike atomic environments act as plasticity carriers in amorphous silicon. *Physical Review B*. 2005;72(24): 245205.
12. Demkowicz MJ, Argon AS, Farkas D, Frary M. Simulation of plasticity in nanocrystalline silicon. *Philosophical Magazine*. 2007;87(28): 4253–4271.
13. Mo YF, Szlufarska I. Simultaneous enhancement of toughness, ductility, and strength of nanocrystalline ceramics at high strain-rates. *Applied Physics Letters*. 2007;90(18): 181926.
14. Pozdnyakov VA, Glezer AM. Structural mechanisms of fracture of nanocrystalline materials. *Physics of the Solid State*. 2005;47(5): 817–824.
15. Skiba NV. Crossover from deformation twinning to lattice dislocation slip in metal–graphene composites with bimodal structures. *Crystals*. 2020;10(1): 47.
16. Gutkin MYu, Skiba NV, Orlova TS. Grain-boundary nanoprecipitates-mediated mechanism of strengthening in Al-Cu-Zr alloy structured by high-pressure torsion. *Materials Physics and Mechanics*. 2022;50(3): 431–438.
17. Smithells CJ, Brands EA. *Metals reference book*. London: Butter-worths; 1976.
18. Munro RG. Evaluated material properties for a sintered α-alumina. *Journal of the American Ceramic Society*. 1997;80(8): 1919–1928.
19. Archer DG. Thermodynamic properties of synthetic sapphire (α-Al_2O_3), standard reference material 720 and the effect of temperature-scale differences on thermodynamic properties. *Journal of Physical and Chemical Reference Data*. 1993;22(6): 1441–1453.
20. Choi S-M, Awaji H. Nanocomposites – a new material design concept. *Science and Technology of Advanced Materials*. 2005;6(1): 2–10.

About Authors

Mikhail Yu. Gutkin
Doctor of Physical and Mathematical Sciences
Head of Department, Principal Researcher (Institute for Problems in Mechanical Engineering RAS, St. Petersburg, Russia)

Nikolay V. Skiba
Doctor of Physical and Mathematical Sciences
Leading Researcher (Institute for Problems in Mechanical Engineering RAS, St. Petersburg, Russia)